

Flavour violating bosonic squark decays at LHC

A. Bartl¹, H. Eberl², E. Ginina¹, B. Herrmann³, K. Hidaka⁴,
W. Majerotto² and W. Porod⁵

¹ *Universität Wien, Fakultät für Physik, A-1090 Vienna, Austria*

² *Institut für Hochenergiephysik der Österreichischen Akademie der Wissenschaften, A-1050 Vienna, Austria*

³ *LAPTh, Université de Savoie, CNRS, 9 Chemin de Bellevue, B.P. 110, F-74941 Annecy-le-Vieux, France*

⁴ *Department of Physics, Tokyo Gakugei University, Koganei, Tokyo 184-8501, Japan*

⁵ *Institut für Theoretische Physik und Astrophysik, Universität Würzburg, D-97074 Würzburg, Germany*

Abstract

We study quark flavour violation (QFV) in the squark sector of the Minimal Supersymmetric Standard Model (MSSM). We assume mixing between the second and the third squark generation i.e. $\tilde{c}_{L,R} - \tilde{t}_{L,R}$ mixing. We focus on QFV effects in bosonic squark decays, in particular in the decay into the lightest Higgs boson, $\tilde{u}_2 \rightarrow \tilde{u}_1 h^0$, where $\tilde{u}_{1,2}$ are the lightest up-type squarks. We show that the branching ratio of this QFV decay can be quite large (up to 60 %) due to large QFV trilinear couplings, and large $\tilde{c}_{L,R} - \tilde{t}_{L,R}$ and $\tilde{t}_L - \tilde{t}_R$ mixing, despite the strong constraints on QFV from B meson data. This can result in remarkable QFV signatures with significant rates at LHC, such as $pp \rightarrow \tilde{g}\tilde{g}X \rightarrow \tilde{u}_{1,2}\tilde{t}\tilde{u}_2\bar{c}X \rightarrow \tilde{u}_{1,2}\tilde{t}\tilde{u}_1h^0\bar{c}X \rightarrow c\tilde{\chi}_1^0\bar{t}c\tilde{\chi}_1^0h^0\bar{c}X (= c\bar{t}c\bar{c}h^0\cancel{E}_TX)$. The QFV bosonic squark decays can have an influence on the squark and gluino searches at LHC and can play a role in the determination of the MSSM parameters, in particular of the QFV trilinear couplings.

1 Introduction

In most searches for supersymmetric (SUSY) particles at the LHC, the analyses have been performed within simplified SUSY models. However, SUSY extensions of the Standard Model (SM) can have a richer structure. In the Minimal Supersymmetric Standard Model (MSSM), mixing between the different squark generations is in principle possible. This could lead to quark flavour violating (QFV) effects, in addition to those induced by the Cabibbo-Kobayashi-Maskawa (CKM) matrix [1, 2, 3]. Mixing between the 1st and the 2nd squark generation is strongly suppressed by K physics data [4]. Therefore, in this paper we assume mixing between the 2nd and the 3rd squark generation, respecting the constraints from B physics (see Appendix B). Although these constraints are also quite severe, they allow nevertheless substantial QFV effects.

In the MSSM, the mixing of the 2nd and the 3rd squark generation was theoretically studied for squark and gluino production and their decays at the LHC in the context of Minimal Flavour Violation (MFV) [5, 6, 7] as well as for general flavour mixing [8, 9, 10, 11, 12, 13, 14, 15]. As shown in these papers the effects of QFV can be large. For example, in the case of mixing between top and charm squarks, we can expect a large branching ratio (up to 40 %) of the QFV decay of the gluino, $\tilde{g} \rightarrow c\bar{t}(\bar{c}t)\tilde{\chi}_1^0$ [13]. This is due to the fact that the lightest up-squark mass eigenstates $\tilde{u}_{1,2}$ are mainly mixtures of \tilde{t}_R and \tilde{c}_R . Hence, \tilde{u}_1 and \tilde{u}_2 can both decay into $c\tilde{\chi}_1^0$ and $t\tilde{\chi}_1^0$.

In addition to the fermionic decays of squarks there are bosonic decays, $\tilde{q}_i \rightarrow \tilde{q}_j + Z^0, h^0, H^0, A^0$ and $\tilde{q}_i \rightarrow \tilde{q}_j' + W^\pm, H^\pm$, if kinematically allowed. In the quark flavour conserving (QFC) case, the most interesting decays are $\tilde{t}_2 \rightarrow \tilde{t}_1 + Z^0, h^0, H^0, A^0$; $\tilde{b}_2 \rightarrow \tilde{b}_1 + Z^0, h^0, H^0, A^0$; $\tilde{b}_2 \rightarrow \tilde{t}_1 + W^-, H^-$. They were studied in [16, 17]. The QFV bosonic decays were recently considered in [11]. There the characteristic differences to the MFV case were worked out. A non-minimal flavour structure in the squark sector can change the entire squark decay pattern quite drastically, because many more transitions are possible.

In the present paper we are particularly interested in the bosonic QFV squark decays into the lightest Higgs boson, $\tilde{q}_i \rightarrow \tilde{q}_j + h^0$ in the MSSM. These decays offer the best possibility of determining the trilinear couplings $\tilde{q}_i - \tilde{q}_j - h^0$ entering the soft-SUSY-breaking Lagrangian. Another possibility would be to study the 3-body production $pp \rightarrow \tilde{q}_i \tilde{q}_j h^0$ as discussed for example in [18] for the QFC case. As the Higgs boson couples dominantly to the $\tilde{q}_L - \tilde{q}_R$ combination, one gets information from the decays $\tilde{q}_i \rightarrow \tilde{q}_j + h^0$ on the flavour structure of the left-right (LR) terms in the squark mass matrix. We shall study the mixing between the 2nd and the 3rd generation of up-type squarks i.e. $\tilde{t}_{L,R} - \tilde{c}_{L,R}$ mixing. There are strong constraints on this mixing from B physics, Higgs boson searches and SUSY particle searches (see Appendix B). In our analysis we take into account all these constraints.

The paper is organized as follows: In Section 2 we shortly give the definitions of the QFV squark mixing parameters. In Section 3 we discuss the QFV bosonic decays of up-type squarks in detail in a definite scenario. We also consider two further scenarios, one GUT inspired and another one where the bosonic decays of \tilde{u}_2 dominate over the fermionic

decays. Section 4 contains a discussion of various QFV signatures. In Section 5 we give a summary. In the Appendices we show explicitly the part of the interaction Lagrangian we use in our analysis and summarize the experimental and theoretical constraints on the MSSM parameters, especially those on the QFV parameters mainly from B physics.

2 Squark mixing with flavour violation

In the MSSM the most general form of the squark mass matrices in the super-CKM basis of $\tilde{q}_{0\gamma} = (\tilde{q}_{1L}, \tilde{q}_{2L}, \tilde{q}_{3L}, \tilde{q}_{1R}, \tilde{q}_{2R}, \tilde{q}_{3R})$, $\gamma = 1, \dots, 6$, with $(q_1, q_2, q_3) = (u, c, t), (d, s, b)$ is [19]

$$\mathcal{M}_{\tilde{q}}^2 = \begin{pmatrix} \mathcal{M}_{\tilde{q},LL}^2 & \mathcal{M}_{\tilde{q},LR}^2 \\ \mathcal{M}_{\tilde{q},RL}^2 & \mathcal{M}_{\tilde{q},RR}^2 \end{pmatrix}, \quad (1)$$

for $\tilde{q} = \tilde{u}, \tilde{d}$, where the 3×3 matrices read

$$\begin{aligned} \mathcal{M}_{\tilde{d},LL}^2 &= M_Q^2 + D_{\tilde{d},LL} \mathbf{1} + \hat{m}_d^2, & \mathcal{M}_{\tilde{u},LL}^2 &= V_{\text{CKM}} M_Q^2 V_{\text{CKM}}^\dagger + D_{\tilde{u},LL} \mathbf{1} + \hat{m}_u^2, \\ \mathcal{M}_{\tilde{d},RR}^2 &= M_D^2 + D_{\tilde{d},RR} \mathbf{1} + \hat{m}_d^2, & \mathcal{M}_{\tilde{u},RR}^2 &= M_U^2 + D_{\tilde{u},RR} \mathbf{1} + \hat{m}_u^2. \end{aligned} \quad (2)$$

Here $M_{Q,U,D}$ are the hermitian soft-SUSY-breaking mass matrices of the squarks and $\hat{m}_{u,d}$ are the diagonal mass matrices of the up-type and down-type quarks. $D_{\tilde{q},LL} = \cos 2\beta m_Z^2 (T_3^q - e_q \sin^2 \theta_W)$ and $D_{\tilde{q},RR} = e_q \sin^2 \theta_W \cos 2\beta m_Z^2$, where T_3^q and e_q are the isospin and electric charge of the quarks (squarks), respectively, and θ_W is the weak mixing angle. The left-left blocks of up-type and down-type squarks are related by the CKM matrix V_{CKM} due to the $SU(2)_L$ symmetry. Note that $V_{\text{CKM}} M_Q^2 V_{\text{CKM}}^\dagger \simeq M_Q^2$ as $V_{\text{CKM}} \simeq 1$. The off-diagonal blocks of eq. (1) read

$$\begin{aligned} \mathcal{M}_{\tilde{d},RL}^2 = \mathcal{M}_{\tilde{d},LR}^{2\dagger} &= \frac{v_1}{\sqrt{2}} T_D^T - \mu^* \hat{m}_d \tan \beta, \\ \mathcal{M}_{\tilde{u},RL}^2 = \mathcal{M}_{\tilde{u},LR}^{2\dagger} &= \frac{v_2}{\sqrt{2}} T_U^T - \mu^* \hat{m}_u \cot \beta, \end{aligned} \quad (3)$$

Here $T_{U,D}^T$ are the transposes of the soft-SUSY-breaking trilinear coupling matrices of the up-type and down-type squarks $T_{U,D}$ defined as $\mathcal{L}_{\text{int}} \supset -(T_{U\alpha\beta} \tilde{u}_{R\beta}^\dagger \tilde{u}_{L\alpha} H_2^0 + T_{D\alpha\beta} \tilde{d}_{R\beta}^\dagger \tilde{d}_{L\alpha} H_1^0)$, μ is the higgsino mass parameter, and $\tan \beta = v_2/v_1$, where $v_{1,2} = \sqrt{2} \langle H_{1,2}^0 \rangle$ are the vacuum expectation values of the neutral Higgs fields. The squark mass matrices are diagonalized by the 6×6 unitary matrices $R^{\tilde{q}}$, $\tilde{q} = \tilde{u}, \tilde{d}$, such that

$$R^{\tilde{q}} \mathcal{M}_{\tilde{q}}^2 (R^{\tilde{q}})^\dagger = \text{diag}(m_{\tilde{q}_1}^2, \dots, m_{\tilde{q}_6}^2) \quad \text{with} \quad m_{\tilde{q}_1} < \dots < m_{\tilde{q}_6}. \quad (4)$$

The physical mass eigenstates $\tilde{q}_i, i = 1, \dots, 6$ are given by $\tilde{q}_i = R_{i\alpha}^{\tilde{q}} \tilde{q}_{0\alpha}$.

We define the QFV parameters in the up-type squark sector $\delta_{\alpha\beta}^{LL}$, $\delta_{\alpha\beta}^{uRR}$ and $\delta_{\alpha\beta}^{uRL}$ ($\alpha \neq \beta$) as follows [20]:

$$\delta_{\alpha\beta}^{LL} \equiv M_{Q\alpha\beta}^2 / \sqrt{M_{Q\alpha\alpha}^2 M_{Q\beta\beta}^2}, \quad (5)$$

$$\delta_{\alpha\beta}^{uRR} \equiv M_{U\alpha\beta}^2 / \sqrt{M_{U\alpha\alpha}^2 M_{U\beta\beta}^2}, \quad (6)$$

$$\delta_{\alpha\beta}^{uRL} \equiv (v_2/\sqrt{2})T_{U\beta\alpha} / \sqrt{M_{U\alpha\alpha}^2 M_{Q\beta\beta}^2}. \quad (7)$$

Here $\alpha, \beta = 1, 2, 3$ ($\alpha \neq \beta$) denote the quark flavours. The QFV parameters relevant for this study are δ_{23}^{uRL} , $\delta_{23}^{uLR} \equiv (\delta_{32}^{uRL})^*$, δ_{23}^{uRR} and δ_{23}^{LL} , which are the $\tilde{c}_R - \tilde{t}_L$, $\tilde{c}_L - \tilde{t}_R$, $\tilde{c}_R - \tilde{t}_R$ and $\tilde{c}_L - \tilde{t}_L$ mixing parameters, respectively. We also use the QFC parameter δ_{33}^{uRL} which is defined by eq. (7) with $\alpha = \beta = 3$ and is the $\tilde{t}_L - \tilde{t}_R$ mixing parameter. We assume all QFV parameters to be real.

3 QFV bosonic decays of up-type squarks

If kinematically allowed, the following QFV bosonic decays of up-type squarks are possible

$$\tilde{u}_i \rightarrow \tilde{u}_j + h^0, H^0, A^0 \quad (8)$$

$$\tilde{u}_i \rightarrow \tilde{d}_j + H^\pm \quad (9)$$

$$\tilde{u}_i \rightarrow \tilde{u}_j + Z^0 \quad (10)$$

$$\tilde{u}_i \rightarrow \tilde{d}_j + W^\pm \quad (11)$$

with $i, j = 1, \dots, 6$ specifying the squark mass eigenstates which are mixtures of the squark flavour eigenstates (see Section 2). Here h^0 (H^0) is the lighter (heavier) CP-even neutral Higgs boson, A^0 is the CP-odd neutral Higgs boson and H^\pm is the charged Higgs boson. Of course, there are also QFC bosonic squark decays. In this article we study mainly $\tilde{u}_{1,2,3}$ decays in scenarios where their decays into charged bosons of eqs. (9) and (11) and those into the heavier Higgs bosons H^0 and A^0 are kinematically forbidden. The couplings between $\tilde{u}_i - \tilde{u}_j/\tilde{d}_j$ and the bosons in eqs. (8) – (11), taking into account QFV, are given in [11]. For completeness, the couplings to the lightest Higgs boson, h^0 , are listed in Appendix A. Note that the QFV parts are proportional to the soft-SUSY-breaking trilinear coupling parameter T_U . In the following discussion of the decays we will adopt the QFV parameters $\delta_{23}^{LL}, \delta_{23}^{uRR}, \delta_{23}^{uRL}, \delta_{23}^{uLR} (= \delta_{32}^{uRL*})$ as defined in Section 2. The parameters $\delta_{23}^{uLR}, \delta_{23}^{uRL}$ are proportional to T_{U23} and T_{U32} , respectively.

In the calculation of the branching ratios of the decays (8) – (11) we have to take into account both QFV and QFC fermionic squark decays [10, 13]

$$\tilde{u}_i \rightarrow u_\alpha + \tilde{\chi}_k^0 \quad (12)$$

$$\tilde{u}_i \rightarrow d_\alpha + \tilde{\chi}_l^\pm \quad (13)$$

$$\tilde{u}_i \rightarrow u_\alpha + \tilde{g} \quad (14)$$

Table 1: Weak scale basic MSSM parameters at $Q = 1$ TeV for Scenario A, except for m_{A^0} which is the pole mass (i.e. the physical mass) of A^0 . All of $T_{U\alpha\alpha}$ and $T_{D\alpha\alpha}$ are zero, except for $T_{U33} = -2160$ GeV (i.e. $\delta_{33}^{uRL} = -0.34$). All other squark parameters not shown here are also zero.

M_1	M_2	M_3	μ	$\tan\beta$	m_{A^0}
400 GeV	800 GeV	1000 GeV	2640 GeV	20	1500 GeV

	$\alpha = 1$	$\alpha = 2$	$\alpha = 3$
$M_{Q\alpha\alpha}^2$	$(2400)^2$ GeV ²	$(2360)^2$ GeV ²	$(1450)^2$ GeV ²
$M_{U\alpha\alpha}^2$	$(2380)^2$ GeV ²	$(780)^2$ GeV ²	$(750)^2$ GeV ²
$M_{D\alpha\alpha}^2$	$(2380)^2$ GeV ²	$(2340)^2$ GeV ²	$(2300)^2$ GeV ²

δ_{23}^{uLL}	δ_{23}^{uRR}	δ_{23}^{uRL}	δ_{23}^{uLR}
0.024	0.3	-0.07	0

Table 2: Physical masses in GeV of the particles in Scenario A (see Table 1).

$m_{\tilde{\chi}_1^0}$	$m_{\tilde{\chi}_2^0}$	$m_{\tilde{\chi}_3^0}$	$m_{\tilde{\chi}_4^0}$	$m_{\tilde{\chi}_1^+}$	$m_{\tilde{\chi}_2^+}$
397	824	2623	2625	825	2625

m_{h^0}	m_{H^0}	m_{A^0}	m_{H^\pm}
126.0	1496	1500	1510

$m_{\tilde{g}}$	$m_{\tilde{u}_1}$	$m_{\tilde{u}_2}$	$m_{\tilde{u}_3}$	$m_{\tilde{u}_4}$	$m_{\tilde{u}_5}$	$m_{\tilde{u}_6}$
1141	605	861	1477	2387	2401	2427

where $\alpha = 1, 2, 3$ is the flavour index, $\tilde{\chi}_k^0, k = 1, \dots, 4$ are the neutralinos and $\tilde{\chi}_l^\pm, l = 1, 2$ are the charginos. As $\tilde{u}_{1,2}$ are mainly mixtures of \tilde{c}_R, \tilde{t}_R and \tilde{t}_L in the scenarios under consideration, both decays $\tilde{u}_{1,2} \rightarrow t\tilde{\chi}_1^0$ and $\tilde{u}_{1,2} \rightarrow c\tilde{\chi}_1^0$ are possible.

In the following we will discuss the QFV bosonic squark decays in three different scenarios. The first one which we call Scenario A and which we will study in detail is shown in Table 1. The corresponding basic SUSY parameters are given at the scale $Q = 1$ TeV according to the SPA convention [21], except for m_{A^0} being the pole mass of A^0 . For this scenario all experimental and theoretical constraints given in Appendix B are satisfied, with the following values of the low energy observables: $\Delta M_{B_s} = 17.2$ ps⁻¹, $B(b \rightarrow s\gamma) = 2.9 \cdot 10^{-4}$, $B(B_s \rightarrow \mu^+\mu^-) = 3.3 \cdot 10^{-9}$. All numerical calculations in this study, except for the cross sections, are performed with the public code SPHeno v3.1 [22, 23]. We also use the package SSP [24]. Further on, we choose relatively large values of M_1, M_2 and μ in order to avoid the dominance of the fermionic squark decays.

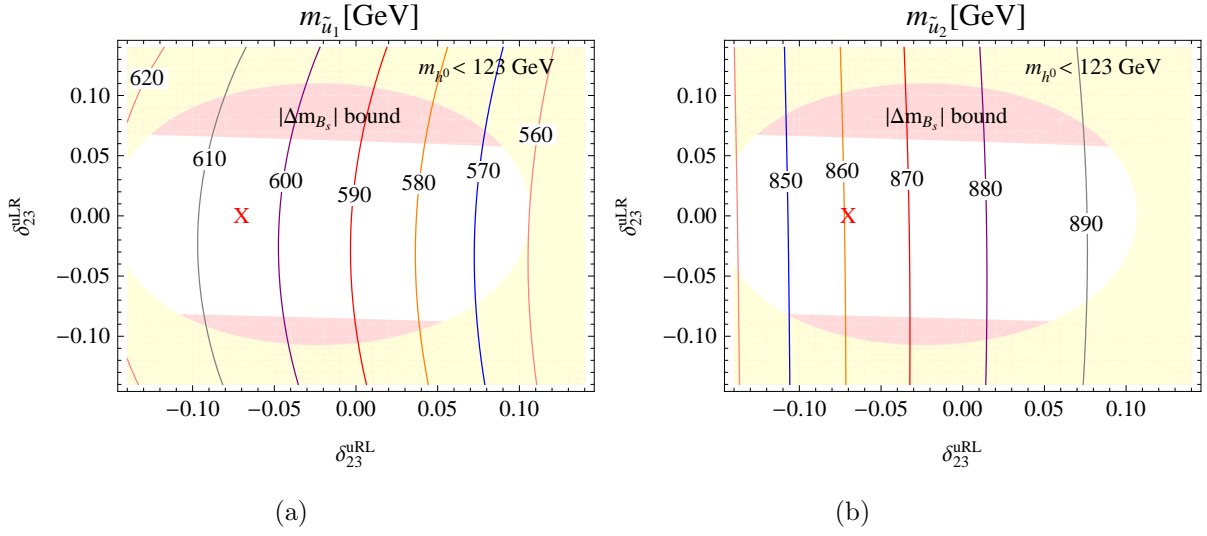


Figure 1: Dependence of the masses of \tilde{u}_1 (a) and \tilde{u}_2 (b) on δ_{23}^{uRL} and δ_{23}^{uLR} in Scenario A, with the parameters given in Table 1. "X" in both plots corresponds to the reference point.

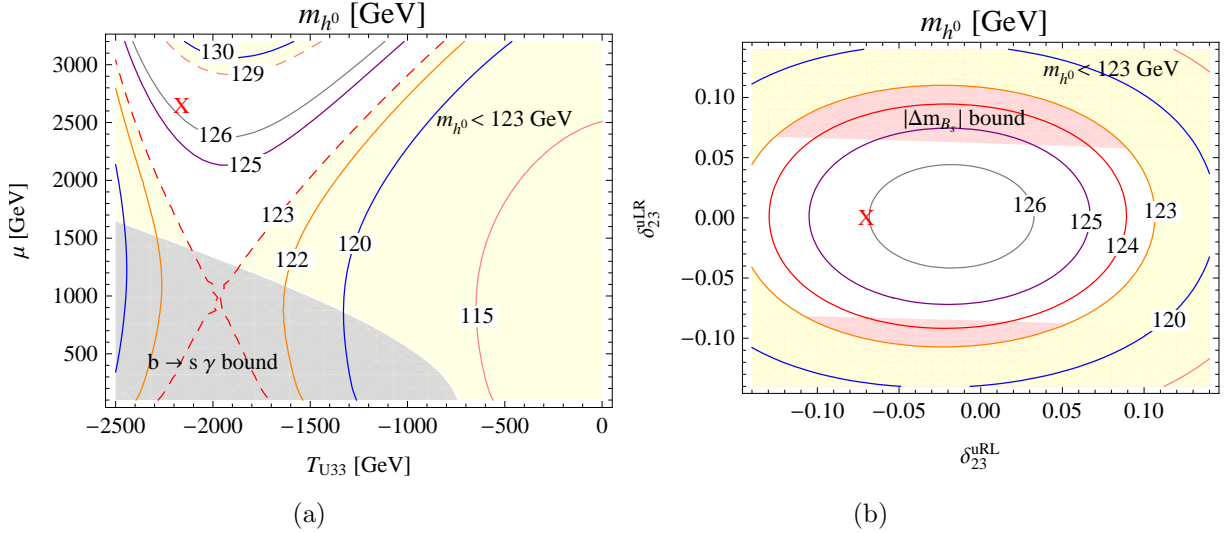


Figure 2: The mass of the lightest Higgs boson, m_{h^0} , as a function of T_{U33} and μ (a) and as a function of δ_{23}^{uRL} and δ_{23}^{uLR} (b) in Scenario A, with the parameters as given in Table 1. "X" corresponds to the reference point in both plots.

M_3 is chosen such that the gluino mass is within the reach of LHC (14 TeV). Note that in the present scenario M_1, M_2 and M_3 do not fulfill gaugino mass unification at the GUT scale. The GUT-inspired case with gaugino mass unification will be studied in a second scenario. The physical masses of squarks, gluino, charginos, neutralinos and Higgs bosons are shown in Table 2. We obtain $m_{h^0} = 126$ GeV which is in the range of the possible Higgs signal at LHC [25] (see Appendix B). Moreover, in this scenario we are in the

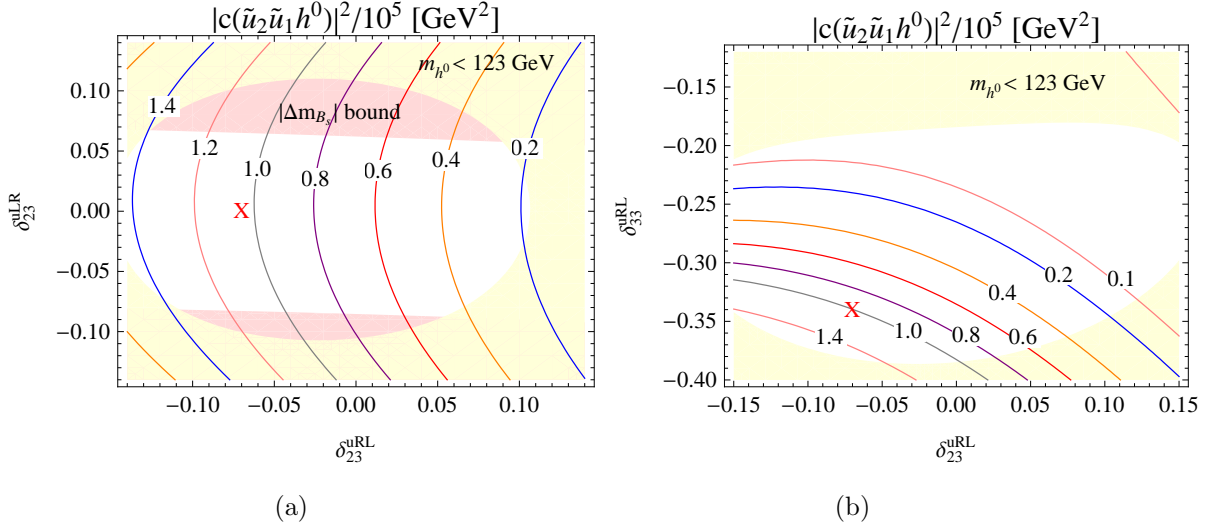


Figure 3: The coupling $|c(\tilde{u}_2\tilde{u}_1h^0)|^2$ as a function of δ_{23}^{uRL} and δ_{23}^{uLR} (a) and as a function of δ_{23}^{uRL} and δ_{33}^{uRL} (b) in Scenario A of Table 1. The reference point is indicated by "X" in both plots.

decoupling limit with $m_{A^0} = 1500$ GeV $\gg m_{h^0}$, and hence the lightest Higgs-boson h^0 is SM like.

In our previous study on QFV fermionic decays of gluinos and squarks it turned out that QFV effects mainly depend on δ_{23}^{uRR} and δ_{23}^{dRR} , whereas the influence of the other QFV parameters was much weaker [10, 13, 14]. In the present paper we concentrate on the dependence of the QFV effects on δ_{23}^{uRL} and δ_{23}^{uLR} , which enter the squark-squark-Higgs couplings.

In Fig. 1(a) and 1(b) we show the mass contours of \tilde{u}_1 and \tilde{u}_2 in the $\delta_{23}^{uRL} - \delta_{23}^{uLR}$ plane. In all contour plots in this article the white regions satisfy all the experimental and theoretical constraints listed in Appendix B. In this scenario with large δ_{23}^{uRR} , δ_{33}^{uRL} and δ_{23}^{uRL} , \tilde{u}_1 is mainly a $\tilde{t}_R - \tilde{c}_R(-\tilde{t}_L)$ mixture and \tilde{u}_2 is mainly a $\tilde{c}_R - \tilde{t}_R(-\tilde{t}_L)$ mixture. One can see a somewhat stronger dependence on δ_{23}^{uRL} due to the sizable mass-splitting induced by the $\tilde{c}_R - \tilde{t}_L$ mixing, which is a consequence of the chosen hierarchy within M_Q^2 and M_U^2 .

In Fig. 2(a) the lightest Higgs mass m_{h^0} is shown as a function of T_{U33} and μ . In order to obtain $m_{h^0} \simeq 126$ GeV a large $|T_{U33}|$ entering the stop loop corrections to m_h^0 and a rather large μ entering the sbottom loop corrections through the term $A_b - \mu \tan \beta$ [26, 27, 28] are required. We have $\mu = 2640$ GeV and $T_{U33} = -2160$ GeV in Scenario A. In Fig. 2(b) we show contours of m_{h^0} in the $\delta_{23}^{uLR} - \delta_{23}^{uRL}$ plane. Within the QFV parameter range shown the m_{h^0} varies by about 3 GeV due to the \tilde{c} admixture in the stop loops.

Next we will study the decay $\tilde{u}_2 \rightarrow \tilde{u}_1 h^0$ in more detail. In Fig. 3(a) we show the squared coupling $|c(\tilde{u}_2\tilde{u}_1h^0)|^2$ (see eq. (17) in Appendix A) as a function of $\delta_{23}^{uRL}(\sim T_{U32})$ and $\delta_{23}^{uLR}(\sim T_{U23})$. Dominant terms in $c(\tilde{u}_2\tilde{u}_1h^0)$ are those proportional to $T_{U33}(= \tilde{t}_R^\dagger - \tilde{t}_L - H_2^0$ coupling) and $T_{U32}(= \tilde{c}_R^\dagger - \tilde{t}_L - H_2^0$ coupling) (see \mathcal{L}_{int} in Section 2) since $\tilde{u}_{1,2}$

are mainly mixtures of \tilde{c}_R , \tilde{t}_R and \tilde{t}_L , and $h^0 \sim \text{Re}(H_2^0)$. Note here that in our scenario there is a large \tilde{c}_R - \tilde{t}_R mixing, $\delta_{23}^{uRR} = 0.3$, a large \tilde{t}_L - \tilde{t}_R mixing, $\delta_{33}^{uRL} = -0.34$. The term proportional to T_{U23} ($= \tilde{t}_R^\dagger - \tilde{c}_L - H_2^0$ coupling) is rather small since the \tilde{c}_L component in $\tilde{u}_{1,2}$ is small mainly due to very large $m_{\tilde{c}_L}$ (~ 2.4 TeV) (see Table 1). The decrease of the $|c(\tilde{u}_2\tilde{u}_1h^0)|^2$ with increase of δ_{23}^{uRL} is due to the fact that the contributions of these two couplings, T_{U33} and T_{U32} , to $c(\tilde{u}_2\tilde{u}_1h^0)$ interfere with each other constructively (destructively) in the case $T_{U33} < 0$ and $T_{U32} < 0$ ($T_{U33} < 0$ and $T_{U32} > 0$). Again the dependence on δ_{23}^{uRL} is much stronger than that on δ_{23}^{uLR} because the contribution of the coupling T_{U23} to $c(\tilde{u}_2\tilde{u}_1h^0)$ is rather small due to the small \tilde{c}_L component in $\tilde{u}_{1,2}$ in our scenario. Fig. 3(b) shows $|c(\tilde{u}_2\tilde{u}_1h^0)|^2$ as a function of the QFV parameter δ_{23}^{uRL} and the QFC parameter δ_{33}^{uLR} with the latter being the $\tilde{t}_L - \tilde{t}_R$ mixing parameter. Also here a strong variation of $|c(\tilde{u}_2\tilde{u}_1h^0)|^2$ can be seen. It increases with increase of $|\delta_{33}^{uRL}|$ since the dominant contribution proportional to T_{U33} in $c(\tilde{u}_2\tilde{u}_1h^0)$ increases because of increasing of both T_{U33} and the \tilde{t}_L component in $\tilde{u}_{1,2}$. The decrease of the $|c(\tilde{u}_2\tilde{u}_1h^0)|^2$ with increase of δ_{23}^{uRL} is due to the same reason as in Fig. 3(a).

In Fig. 4(a) we show the branching ratio of the decay $\tilde{u}_2 \rightarrow \tilde{u}_1h^0$ as a function of the QFV parameters δ_{23}^{uRL} and δ_{23}^{uLR} . This branching ratio can exceed 50%. Analogous to Fig. 3(a), the dependence on δ_{23}^{uRL} is stronger than that on δ_{23}^{uLR} . In Fig. 4(b) we show the bosonic \tilde{u}_2 decay branching ratio $B(\tilde{u}_2 \rightarrow \tilde{u}_1h^0)$ in the δ_{23}^{uRL} - δ_{33}^{uRL} plane. Its dependence on δ_{23}^{uRL} and δ_{33}^{uRL} can be explained by that of $|c(\tilde{u}_2\tilde{u}_1h^0)|^2$ shown in Fig. 3(b). The branching ratio $B(\tilde{u}_2 \rightarrow \tilde{u}_1h^0)$ can go up to 60% satisfying all relevant experimental and theoretical constraints listed in Appendix B. At the reference point of Table 1 it is about 46%. Note that at this point $B(\tilde{u}_2 \rightarrow c\tilde{\chi}_1^0) \simeq 40\%$ and $B(\tilde{u}_2 \rightarrow t\tilde{\chi}_1^0) \simeq 10\%$ whereas $B(\tilde{u}_2 \rightarrow \tilde{u}_1Z^0)$ is very small ($\approx 1\%$). Note also that QFV effects (mainly due to the $\tilde{c}_R - \tilde{t}_R$ mixing and the $\tilde{c}_R - \tilde{t}_L$ mixing ($\sim T_{U32}$)) together with the large top trilinear coupling T_{U33} ($\sim \tilde{t}_R - \tilde{t}_L$ mixing parameter) can lead to a strongly enhanced branching ratio for the \tilde{u}_2 decay into h^0 .

We have also studied the QFV decays $\tilde{u}_3 \rightarrow \tilde{u}_1h^0$ and $\tilde{u}_3 \rightarrow \tilde{u}_2h^0$. The branching ratio of $\tilde{u}_3 \rightarrow \tilde{u}_1h^0$ can go up to 30%. At the reference point of Table 1 is about 22%. \tilde{u}_3 has a large \tilde{t}_L component hence the $\tilde{u}_3 \rightarrow \tilde{u}_1h^0$ transitions are mainly due to $\tilde{t}_L \rightarrow \tilde{t}_Rh^0$. On the other hand, in the decay $\tilde{u}_3 \rightarrow \tilde{u}_2h^0$ the behaviour of the branching ratio is very different, because the $\tilde{t}_L - \tilde{c}_R$ transitions are more important. Its branching ratio at the reference point is about 10%. The branching ratios of $\tilde{u}_3 \rightarrow \tilde{u}_1Z^0$ and $\tilde{u}_3 \rightarrow \tilde{u}_2Z^0$ at the reference point are about 28% and 14%, respectively.

In Scenario A the squark \tilde{u}_2 can also be produced in the decay of the gluino. We show in Fig. 5(a) and 5(b) the branching ratios of the decays $\tilde{g} \rightarrow \tilde{u}_2\bar{c} + c.c.$ and $\tilde{g} \rightarrow \tilde{u}_2\bar{t} + c.c.$ as functions of δ_{23}^{uRL} and δ_{33}^{uRL} . The branching ratio of the decay $\tilde{g} \rightarrow \tilde{u}_2\bar{t} + c.c.$ is much smaller than that of $\tilde{g} \rightarrow \tilde{u}_2\bar{c} + c.c.$ due to phase space.

Furthermore, we have studied a scenario (Scenario B) where the gaugino mass parameters M_1 , M_2 and M_3 obey the GUT relation $M_1 \approx 0.5 M_2$, $M_3/M_2 = g_3^2/g_2^2$, where g_2 and g_3 are the SU(2) and SU(3) gauge coupling constants, respectively. More definitely, we have changed only M_1 , M_2 , and M_3 with respect to the values of Table 1, leaving all other parameters unchanged. We choose $M_1 = 250$ GeV, which leads to $M_2 = 500$ GeV

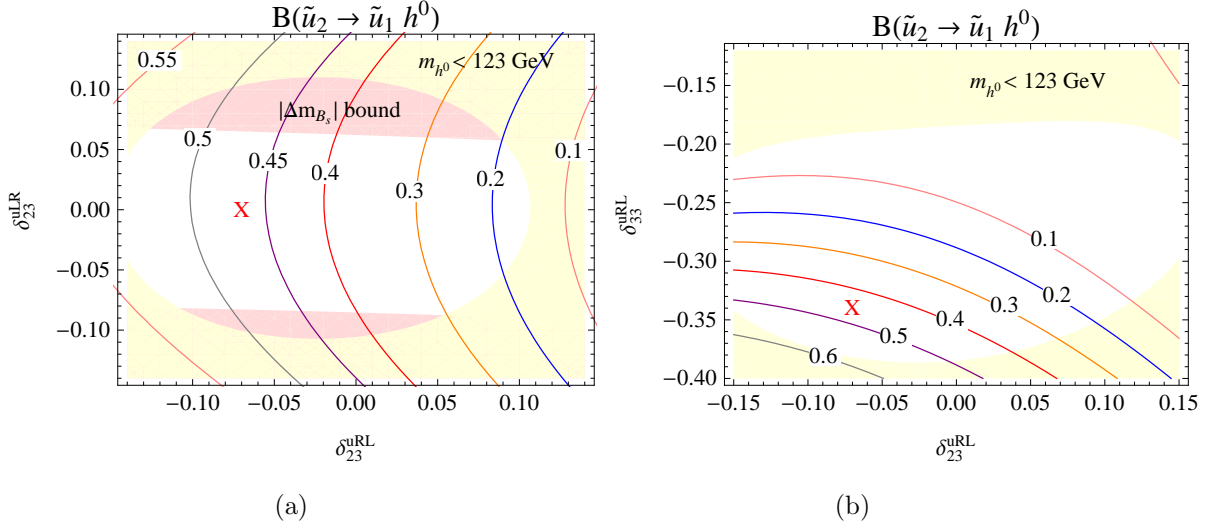


Figure 4: The branching ratio of the decay $\tilde{u}_2 \rightarrow \tilde{u}_1 h^0$ as a function of δ_{23}^{uRL} and δ_{23}^{uLR} (a) and as a function of δ_{23}^{uRL} and δ_{33}^{uRL} (b) in Scenario A, with parameters as shown in Table 1. In both plots "X" indicates the reference point.

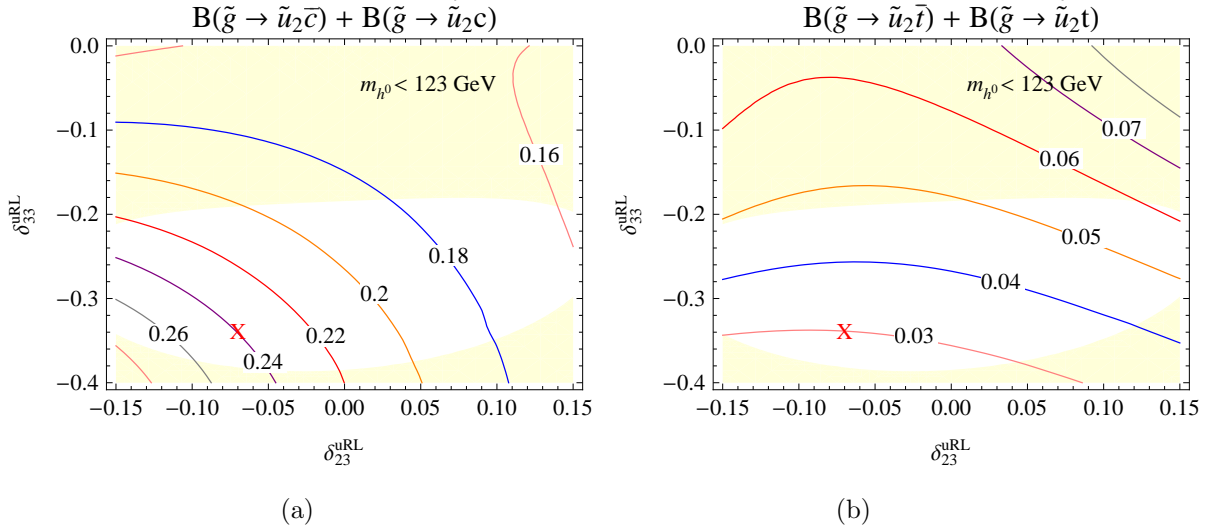


Figure 5: The branching ratios $B(\tilde{g} \rightarrow \tilde{u}_2 \bar{c}) + B(\tilde{g} \rightarrow \tilde{u}_2 c)$ (a) and $B(\tilde{g} \rightarrow \tilde{u}_2 \bar{t}) + B(\tilde{g} \rightarrow \tilde{u}_2 t)$ (b) as functions of δ_{23}^{uRL} and δ_{33}^{uRL} in Scenario A. The corresponding parameters are given in Table 1. "X" indicates the reference point in both plots.

and $M_3 = 1500 \text{ GeV}$. The physical masses of the squarks are almost the same as in Table 2. In this scenario the gluino is relatively heavy, $m_{\tilde{g}} = 1626 \text{ GeV}$, therefore, it has a relatively small production cross section $pp \rightarrow \tilde{g}\tilde{g}X$. As we will see in the next section, gluino production is important, because the lighter squarks $\tilde{u}_{1,2}$ are also produced in the gluino decays $\tilde{g} \rightarrow \tilde{u}_{1,2} \bar{q}$. Concerning the mass of the h^0 , the coupling $|c(\tilde{u}_1 \tilde{u}_2 h^0)|^2$ and

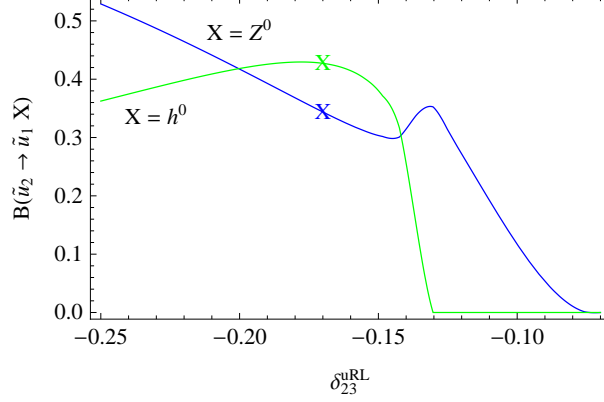


Figure 6: δ_{23}^{uRL} dependence of the branching ratios $B(\tilde{u}_2 \rightarrow \tilde{u}_1 h^0)$ and $B(\tilde{u}_2 \rightarrow \tilde{u}_1 Z^0)$ in Scenario C. "X" indicates the reference point defined with the parameters of Table 1, except for those shown in eq. (15). The vanishing of $B(\tilde{u}_2 \rightarrow \tilde{u}_1 h^0)$ at $\delta_{23}^{uRL} \approx -0.13$ is due to kinematics, which also causes the peak of $B(\tilde{u}_2 \rightarrow \tilde{u}_1 Z^0)$.

the branching ratio $\tilde{u}_2 \rightarrow \tilde{u}_1 h^0$, they are very similar to those shown in Figs. 2, 3, and 4.

In exploring various scenarios we have also studied one (Scenario C) where the QFV bosonic squark decays $\tilde{u}_2 \rightarrow \tilde{u}_1 h^0$ and $\tilde{u}_2 \rightarrow \tilde{u}_1 Z^0$ dominate over the fermionic \tilde{u}_2 decays. We have again changed some of the MSSM parameters with respect to Table 1, leaving all other parameters unchanged,

$$\begin{aligned} M_{U22}^2 &= (650 \text{ GeV})^2, & M_{U33}^2 &= (1600 \text{ GeV})^2, & M_{Q33}^2 &= (780 \text{ GeV})^2, \\ \delta_{23}^{uLL} &= 0, & \delta_{23}^{uRR} &= 0, & \delta_{23}^{uRL} &= -0.17, & \delta_{33}^{uRL} &= -0.3. \end{aligned} \quad (15)$$

In particular, the QFV trilinear coupling parameter $\delta_{23}^{uRL} (\sim T_{U32})$ is much larger than that in Scenario A. This new scenario satisfies all experimental and theoretical constraints listed in Appendix B. For the physical masses and branching ratios, we obtain the following results: $m_{\tilde{g}} = 1134 \text{ GeV}$, $m_{\tilde{u}_1} = 651 \text{ GeV}$, $m_{\tilde{u}_2} = 800 \text{ GeV}$, $m_{\tilde{u}_3} = 1580 \text{ GeV}$, $m_{h^0} = 125.3 \text{ GeV}$, $m_{\tilde{\chi}_1^0} = 398 \text{ GeV}$, $B(\tilde{u}_2 \rightarrow \tilde{u}_1 h^0) = 43\%$, $B(\tilde{u}_2 \rightarrow \tilde{u}_1 Z^0) = 34\%$, $B(\tilde{g} \rightarrow \tilde{u}_2 \bar{c}) + B(\tilde{g} \rightarrow \tilde{u}_2 c) = 8\%$, $B(\tilde{g} \rightarrow \tilde{u}_2 \bar{t}) + B(\tilde{g} \rightarrow \tilde{u}_2 t) = 15\%$, $B(\tilde{u}_1 \rightarrow \tilde{\chi}_1^0 c) = 96\%$, $B(\tilde{u}_1 \rightarrow \tilde{\chi}_1^0 t) = 4\%$. Note that both $B(\tilde{u}_2 \rightarrow \tilde{u}_1 h^0)$ and $B(\tilde{u}_2 \rightarrow \tilde{u}_1 Z^0)$ are very large, leading to the dominance of the QFV bosonic decays of \tilde{u}_2 . Note also that $\tilde{u}_{1,2}$ are mixtures of \tilde{c}_R and \tilde{t}_L due to the sizable QFV trilinear coupling $T_{U32} (= (\tilde{c}_R^\dagger - \tilde{t}_L - H_2^0 \text{ coupling}) \sim \delta_{23}^{uRL})$, which significantly enhances the QFV decay $\tilde{u}_2 \rightarrow \tilde{u}_1 h^0$. The large $B(\tilde{u}_2 \rightarrow \tilde{u}_1 Z^0)$ is mainly due to the sizable \tilde{t}_L component in $\tilde{u}_{1,2}$ in this scenario whereas in Scenario A the \tilde{t}_L component is small. In Fig. 6 we show $B(\tilde{u}_2 \rightarrow \tilde{u}_1 Z^0)$ and $B(\tilde{u}_2 \rightarrow \tilde{u}_1 h^0)$ as functions of δ_{23}^{uRL} . We see that the ratio $B(\tilde{u}_2 \rightarrow \tilde{u}_1 Z^0)/B(\tilde{u}_2 \rightarrow \tilde{u}_1 h^0)$ is sensitive to the QFV as well as to the QFC SUSY parameters.

4 Signatures

In this section we will work out the signatures to be expected from the QFV decays of \tilde{u}_2 into the lightest Higgs boson h^0 within the scenarios considered. The lighter squark states can be produced directly, $pp \rightarrow \tilde{u}_1 \tilde{u}_1 X$, $pp \rightarrow \tilde{u}_2 \tilde{u}_2 X$, or via gluino production, $pp \rightarrow \tilde{g} \tilde{g} X$, where at least one of the gluino decays into \tilde{u}_1 or \tilde{u}_2 , $\tilde{g} \rightarrow \tilde{u}_{1,2} u$; $\tilde{u}_{1,2} c$; $\tilde{u}_{1,2} t$, with q being a light quark. In Table 3 we list the QFV processes leading to at least one Higgs boson h^0 in the final state. We assume that the t -quark can be identified, but the c -quark not. Of course, additional c -tagging would be very helpful. In the following t denotes top-quark or anti-top-quark. What concerns the final states from $\tilde{u}_2 \tilde{u}_2$ pair production, the final states with one t are explicit QFV signals whereas those with no t and $2t$ are apparent QFC signals. Concerning the final states from gluino pair production, those with one t and $3t$ are explicit QFV signals whereas those with no t and $4t$ are apparent QFC signals; those with $2t$ are explicit QFV (apparent QFC) signals in case they are "top-quark top-quark" ("top-quark anti-top-quark"). Note here that the final states with "top-quark anti-top-quark" can stem from both QFV and QFC gluino decays, e.g. $\tilde{g} \tilde{g} \rightarrow (c \bar{t} h^0 \tilde{\chi}_1^0) + (t \bar{c} h^0 \tilde{\chi}_1^0)$ and $\tilde{g} \tilde{g} \rightarrow (t \bar{t} h^0 \tilde{\chi}_1^0) + (c \bar{c} h^0 \tilde{\chi}_1^0)$. Note also that the signal events with tt (or $t\bar{t}$) jj , such as tt (or $t\bar{t}$) $jj h^0 \cancel{E}_T X$, can practically not be produced in the QFC MSSM (nor in the SM). Because of the tiny SM background the detection of such di-top-quark signal events could be useful for discriminating between the QFC MSSM and QFV MSSM.

At $\sqrt{s} = 14$ TeV, for Scenario A, the production cross section for $pp \rightarrow \tilde{g} \tilde{g} X$ is 148 fb including one-loop SUSY-QCD corrections. For that we used Prospino2 [29] as this cross section is only very weakly dependent on the QFV parameters. The cross sections for $pp \rightarrow \tilde{u}_2 \tilde{u}_2 X$, $pp \rightarrow \tilde{g} \tilde{u}_1 X$, and $pp \rightarrow \tilde{g} \tilde{u}_2 X$ are at tree-level 10 fb, 1 fb, and 1.4 fb, respectively. For the calculation of these cross sections we have used FeynArts and FormCalc [30, 31]. All numbers for the signal cross sections given in this section include the charge conjugate final states.

In Scenario A, at the reference point (see Table 1), the branching ratio for $\tilde{u}_2 \rightarrow \tilde{u}_1 h^0$ is about 47% and that for $\tilde{u}_2 \rightarrow \tilde{u}_1 Z^0$ is about 1%. We also have $B(\tilde{u}_1 \rightarrow c \tilde{\chi}_1^0) = 36\%$, $B(\tilde{u}_1 \rightarrow t \tilde{\chi}_1^0) = 64\%$, $B(\tilde{u}_2 \rightarrow c \tilde{\chi}_1^0) = 43\%$, $B(\tilde{u}_2 \rightarrow t \tilde{\chi}_1^0) = 9\%$. Therefore the produced $\tilde{u}_2 \tilde{u}_2$ state goes with a probability of roughly 15% into the final state $2j + h^0 + \cancel{E}_T$. In our scenario, the corresponding cross section for $pp \rightarrow \tilde{u}_2 \tilde{u}_2 X \rightarrow 2j + h^0 + \cancel{E}_T + X$ is almost 1.5 fb. Note, however, that this signature can also occur in the QFC bosonic decays. On the other hand, the process $pp \rightarrow \tilde{u}_2 \tilde{u}_2 X \rightarrow j + t + h^0 + \cancel{E}_T + X$ is QFV and the corresponding cross section is almost 2.8 fb. Even the cross section for $pp \rightarrow \tilde{u}_2 \tilde{u}_2 X \rightarrow j + t + 2h^0 + \cancel{E}_T + X$ is about 1 fb. As the ratio $B(\tilde{u}_2 \rightarrow \tilde{u}_1 Z^0) / B(\tilde{u}_2 \rightarrow \tilde{u}_1 h^0)$ is only about 0.02 at the reference point, the signature $\tilde{u}_2 \tilde{u}_2 \rightarrow 2j + Z^0 + h^0 + \cancel{E}_T$ has a probability of only 0.1%.

The squarks \tilde{u}_2 are also produced in gluino decays. The branching ratios for the gluino decays at the reference point of Scenario A are $B(\tilde{g} \rightarrow \tilde{u}_1 \bar{c} + c.c.) = 18\%$, $B(\tilde{g} \rightarrow \tilde{u}_1 \bar{t} + c.c.) = 55\%$, $B(\tilde{g} \rightarrow \tilde{u}_2 \bar{c} + c.c.) = 24\%$ and $B(\tilde{g} \rightarrow \tilde{u}_2 \bar{t} + c.c.) = 3\%$. For the process $\tilde{g} \tilde{g} \rightarrow \tilde{u}_2 \tilde{u}_2 jj \rightarrow 4j + h^0 + \cancel{E}_T + X$ one gets, therefore, a probability of 0.8%, leading to a cross section for $pp \rightarrow \tilde{g} \tilde{g} X \rightarrow \tilde{u}_2 \tilde{u}_2 jj X \rightarrow 4j + h^0 + \cancel{E}_T + X$ of about 1.2 fb. In

Table 3: Possible signatures expected from the QFV decays of \tilde{u}_2 into the lightest Higgs boson h^0 . t denotes top-quark or anti-top-quark; j denotes a c -quark jet. We also give the cross section to be expected in Scenario A, in case it exceeds 1 fb.

processes	final states containing h^0
$pp \rightarrow \tilde{u}_2 \bar{\tilde{u}}_2 X$	$2j + h^0 + \cancel{E}_T + X$ (1.4 fb) $j + t + h^0 + \cancel{E}_T + X$ (2.8 fb) $j + t + 2h^0 + \cancel{E}_T + X$ (1 fb) $2j + Z^0 + h^0 + \cancel{E}_T + X$ $2j + 2h^0 + \cancel{E}_T + X$ $2t + h^0 + \cancel{E}_T + X$ $2t + 2h^0 + \cancel{E}_T + X$
processes	final states containing h^0
$pp \rightarrow \tilde{g} \tilde{g} X$	$4j + h^0 + \cancel{E}_T + X$ (2 fb) $3j + t + h^0 + \cancel{E}_T + X$ (8 fb) $2j + 2t + h^0 + \cancel{E}_T + X$ (4 fb) $4j + Z^0 + h^0 + \cancel{E}_T + X$ $4j + 2h^0 + \cancel{E}_T + X$ $3j + t + 2h^0 + \cancel{E}_T + X$ $2j + 2t + 2h^0 + \cancel{E}_T + X$ $3j + t + Z^0 + h^0 + \cancel{E}_T + X$ $2j + 2t + Z^0 + h^0 + \cancel{E}_T + X$ $4t + h^0/Z^0(+h^0/Z^0) + \cancel{E}_T + X$

the process $pp \rightarrow \tilde{g} \tilde{g} X \rightarrow \tilde{u}_2 \tilde{u}_2 jj X$ the final state $4j + 2h^0 + \cancel{E}_T + X$ is possible with a probability of approximately 0.3%. The cross section for $pp \rightarrow \tilde{g} \tilde{g} X \rightarrow 4j + 2h^0 + \cancel{E}_T + X$ is 0.5 fb.

A further interesting process is $pp \rightarrow \tilde{g} \tilde{g} X \rightarrow \tilde{u}_1 \tilde{u}_2 jj X \rightarrow 4j + h^0 + \cancel{E}_T + X$, having a probability of 0.5%, giving a cross section of 0.8 fb. Therefore, one has a cross section of 2 fb altogether for $pp \rightarrow \tilde{g} \tilde{g} X \rightarrow 4j + h^0 + \cancel{E}_T + X$. The QFV final state $3j + t + h^0 + \cancel{E}_T + X$ coming from $pp \rightarrow \tilde{g} \tilde{g} X$ has a cross section of 8 fb. Correspondingly, the final state $2j + 2t + h^0 + \cancel{E}_T + X$ from $pp \rightarrow \tilde{g} \tilde{g} X$ has a cross section of 4 fb and that of $pp \rightarrow \tilde{g} \tilde{g} X \rightarrow 3j + t + 2h^0 + \cancel{E}_T + X$ is almost 0.9 fb. We give in Table 3 the cross sections corresponding to the final states as discussed. All other final states shown have cross sections smaller than 1 fb.

Summing up the cross sections for all QFV final states with at least one h^0 one gets

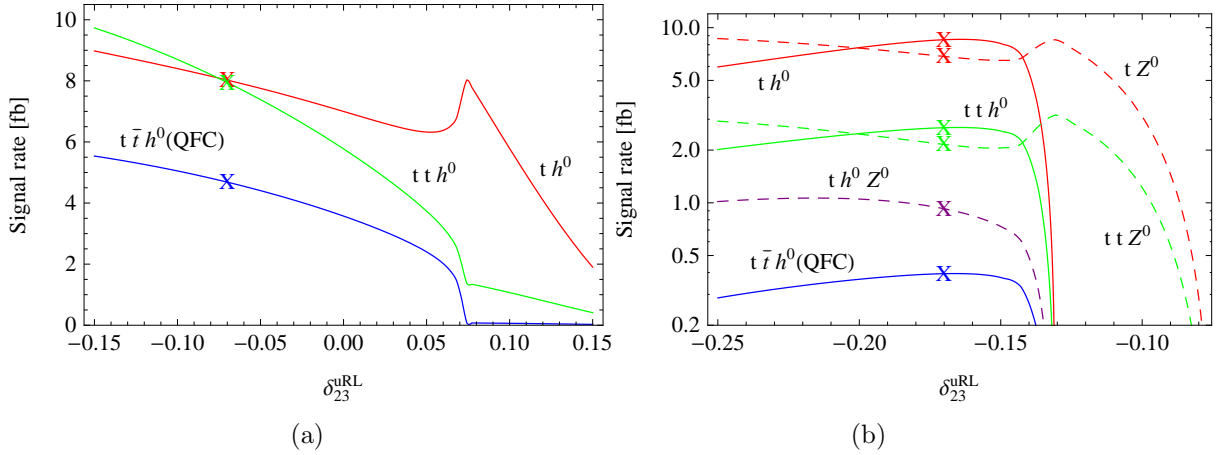


Figure 7: Signal rates for the QFV bosonic squark decay signatures from gluino pair production (a) in Scenario A and (b) in Scenario C as functions of δ_{23}^{uRL} . The red solid (dashed) line corresponds to the pure QFV one t final state $3j + t + h^0$ (Z^0) + $\cancel{E}_T + X$. The green solid (dashed) line corresponds to the QFV signal events with $2t$ coming from $tt/\bar{t}\bar{t} + 2j + h^0$ (Z^0) + $\cancel{E}_T + X$. The blue solid line corresponds to the QFC signal events $t + \bar{t} + 2j + h^0$ + $\cancel{E}_T + X$. The violet dashed line corresponds to the pure QFV one t final state $3j + t + h^0 + Z^0$ + $\cancel{E}_T + X$. Note that the final states containing Z^0 are not so important in Scenario A and therefore not shown in (a). "X" indicates the corresponding scenario's reference point: for Scenario A defined with the parameters of Table 1, and for Scenario C defined with the parameters of Table 1, except for those shown in eq. (15).

19 fb in the scenario considered. This means that one could expect about 1900 of such events assuming an integrated luminosity of 100 fb^{-1} .

In Fig. 7(a) we show the signal cross sections for $pp \rightarrow \tilde{g}\tilde{g}X \rightarrow 3j + t + h^0 + \cancel{E}_T + X$ and $pp \rightarrow \tilde{g}\tilde{g}X \rightarrow 2j + 2t + h^0 + \cancel{E}_T + X$ in Scenario A as a function of δ_{23}^{uRL} . The red solid line corresponds to the pure QFV one t final state $3j + t + h^0 + \cancel{E}_T + X$. The green solid line corresponds to the pure QFV $2t$ final state $tt/\bar{t}\bar{t} + 2j + h^0 + \cancel{E}_T + X$ plus the $2t$ final state signal coming from QFV gluino decays, $t\bar{t} + 2j + h^0 + \cancel{E}_T + X$. Note that the contribution of the $tt/\bar{t}\bar{t}$ final state events is exactly equal to the contribution of the QFV $t\bar{t}$ final state events due to the Majorana nature of the gluino. The blue solid line corresponds to the QFC signal events $t + \bar{t} + 2j + h^0 + \cancel{E}_T + X$ coming from the QFC gluino decays. The behaviour at $\delta_{23}^{uRL} = 0.074$ is due to the fact that the decay $\tilde{u}_1 \rightarrow t\tilde{\chi}_1^0$ is kinematically not possible whereas the decay $\tilde{u}_2 \rightarrow t\tilde{\chi}_1^0$ is still allowed (with 18% branching ratio). Note that the QFV cross sections do not vanish for $\delta_{23}^{uRL} = 0$ because the other QFV parameters δ_{23}^{uLL} and δ_{23}^{uRR} are not zero.— In the GUT inspired scenario (Scenario B) the gluino is much heavier and therefore the cross section $\sigma(pp \rightarrow \tilde{g}\tilde{g}X)$ is much smaller being 3.5 fb. The final state coming from $pp \rightarrow \tilde{u}_2\tilde{u}_2X$ have the same cross section as in scenario A whereas the final states due to $pp \rightarrow \tilde{g}\tilde{g}X$ are about a factor of 40 smaller.

The third scenario (Scenario C) is characterized by a higher branching ratio $B(\tilde{u}_2 \rightarrow \tilde{u}_1 Z^0) = 34\%$. Therefore, one expects final states with Z^0 and h^0 . As the gluino mass is

very close to that of Scenario A, the cross section for $pp \rightarrow \tilde{g}\tilde{g}X$ is 148 fb. Consequently, the cross section $\sigma(pp \rightarrow \tilde{g}\tilde{g}X \rightarrow 3j + t + h^0 + \cancel{E}_T + X)$ is 8.5 fb and $\sigma(pp \rightarrow \tilde{g}\tilde{g}X \rightarrow 3j + t + Z^0 + \cancel{E}_T + X)$ is 6.8 fb. In Fig. 7(b) we show the cross sections analogous to those shown in Fig. 7(a), but for Scenario C. In addition, we also show the cross sections of the QFV final states containing Z^0 . The green dashed line corresponds to the pure QFV $2t$ final state $t\bar{t}/t\bar{t} + 2j + Z^0 + \cancel{E}_T + X$ plus the $2t$ final state signal coming from QFV gluino decays, $t\bar{t} + 2j + Z^0 + \cancel{E}_T + X$. The contribution of the $t\bar{t}/t\bar{t}$ final state events is again equal to the contribution of the QFV $t\bar{t}$ final state events. The violet dashed line corresponds to pure QFV one t final state $3j + t + h^0 + Z^0 + \cancel{E}_T + X$. Fig. 7(b) is symmetric in $\delta_{23}^{uRL} \rightarrow -\delta_{23}^{uRL}$.

We want to comment shortly on the background coming from SM processes and MSSM processes. In the SM the main background is the production of a Higgs boson H in association with top quarks, $pp \rightarrow t\bar{t}HX$, where H is radiated off from top or antitop. The cross section at $\sqrt{s} = 14$ TeV is about 400 fb. In these events, however, there is no missing energy, \cancel{E}_T . Further Higgs boson production processes are $pp \rightarrow Z^0 Z^0 H; W^+ W^- H$. They will of course, constitute a background to the $h^0 + jets + \cancel{E}_T$. However, these processes do not contain a top in the final state. As discussed above, events with top (antitop) in the final states together with a h^0 are the most significant signatures for QFV. Single H production via top loops in gluon-gluon fusion as well as $pp \rightarrow b\bar{b}HX$ do not contain a top quark in the final state either.

As we have shown, the final state with $t + h^0 + jets$ has the largest cross section in the scenarios considered. Concerning the background within the general MSSM, the situation can be more complex. In the scenarios considered the charginos and neutralinos are relatively heavy, so that the decays of the lightest squarks $\tilde{u}_{1,2}$ into these play a minor role, except those into the lightest neutralino. If this is not the case the QFV signals will be less pronounced. Clearly MC studies including detector effects and appropriate cuts would be necessary to select the proposed QFV signals. However, this is beyond the scope of this paper.

5 Summary

In this paper we have studied the effects of QFV in the bosonic squark decays $\tilde{u}_2 \rightarrow \tilde{u}_1 h^0/Z^0$ and $\tilde{u}_3 \rightarrow \tilde{u}_{1,2} h^0/Z^0$ at the LHC. We have assumed mixing between the second and third squark generations, that is $\tilde{c}_{L,R} - \tilde{t}_{L,R}$ mixing. In our calculations we have taken into account all experimental constraints from B meson data on ΔM_{B_s} , $B(b \rightarrow s\gamma)$, $B(B_s \rightarrow \mu\mu)$, limits on the gluino and squark masses, the latest data on the lightest Higgs boson mass, $m_{h^0} \approx 126$ GeV, and the theoretical constraints on the trilinear couplings from the vacuum stability conditions. We have found that the branching ratio $B(\tilde{u}_2 \rightarrow \tilde{u}_1 h^0)$ can be larger than in the QFC case, and can go up to 60%, and that the decay $\tilde{u}_2 \rightarrow \tilde{u}_1 h^0$ gives access to the QFV trilinear couplings T_{U32} and T_{U23} . We have studied the signatures expected from the QFV decay $\tilde{u}_2 \rightarrow \tilde{u}_1 h^0$ at LHC with $\sqrt{s} = 14$ TeV in three different scenarios. We have considered direct \tilde{u}_2 production $pp \rightarrow \tilde{u}_2 \tilde{u}_2 X$ as well

as \tilde{u}_2 production in \tilde{g} decays via $pp \rightarrow \tilde{g}\tilde{g}X$. In two scenarios (A and C) we have taken $m_{\tilde{g}} \approx 1100$ GeV and $m_{\tilde{u}_2} \approx 860$ GeV and in the third scenario (B) $m_{\tilde{g}} \approx 1600$ GeV. The most pronounced QFV signature is $3j + t + h^0 + \cancel{E}_T + X$, for example coming from $pp \rightarrow \tilde{g}\tilde{g}X \rightarrow \tilde{u}_{1,2}\bar{t}\tilde{u}_2\bar{c}X \rightarrow \tilde{u}_{1,2}\bar{t}\tilde{u}_1h^0\bar{c}X \rightarrow c\bar{t}c\bar{c}h^0\cancel{E}_TX$, which can have a cross section up to 8 fb in Scenario A. A further interesting QFV signature coming from gluino pair production is $2j + 2t + h^0 + \cancel{E}_T + X$ with a cross section in Scenario A of about 4 fb.

In conclusion, our analysis suggests that for a complete determination of the MSSM parameters it will be necessary to study both the fermionic and the bosonic QFC and QFV decays of squarks. This can also have an influence on the squark and gluino searches at LHC.

Acknowledgments

This work is supported by the "Fonds zur Förderung der wissenschaftlichen Forschung (FWF)" of Austria, project No. I 297-N16 and by the DFG, project No. PO-1337/2-1.

A Up-squark decay into h^0

In the super-CKM basis, the Lagrangian including the coupling of up-type squarks to the lighter neutral Higgs boson, h^0 , is given by

$$\begin{aligned} \mathcal{L} = & -\frac{g_2}{2m_W} h^0 \left[\tilde{u}_{iL}^* \tilde{u}_{jL} \left(m_W^2 \sin(\alpha + \beta) \left(1 - \frac{1}{3} \tan^2 \theta_W \right) \delta_{ij} + 2 \frac{\cos \alpha}{\sin \beta} m_{u,i}^2 \delta_{ij} \right) \right. \\ & + \tilde{u}_{iR}^* \tilde{u}_{jR} \left(m_W^2 \sin(\alpha + \beta) \frac{4}{3} \tan^2 \theta_W \delta_{ij} + 2 \frac{\cos \alpha}{\sin \beta} m_{u,i}^2 \delta_{ij} \right) \\ & \left. + \left[\tilde{u}_{iR}^* \tilde{u}_{jL} \left(\mu^* \frac{\sin \alpha}{\sin \beta} m_{u,i} \delta_{ij} + \frac{\cos \alpha}{\sin \beta} \frac{v_2}{\sqrt{2}} (T_U)_{ji} \right) + \text{h.c.} \right] \right]. \end{aligned} \quad (16)$$

The terms going with m_W^2 stem from the D-terms of the scalar potential and the expressions with quark masses $m_{u,d}$ stem from Yukawa and F-terms. They are all flavour-universal. The trilinear couplings are explicit breaking terms that couple left-handed to right-handed squarks. Inserting the transformations to the physical fields, $\tilde{u}_{iL} = (R^{\tilde{u}\dagger})_{ik} \tilde{u}_k$ and $\tilde{u}_{iR} = (R^{\tilde{u}\dagger})_{(i+3)k} \tilde{u}_k$, eq. (16) can be written in terms of physical up-type squark fields

as $\mathcal{L} = c_{\tilde{u}_i \tilde{u}_j h^0} \tilde{u}_j^* \tilde{u}_i h^0$ with the coupling

$$\begin{aligned}
c_{\tilde{u}_i \tilde{u}_j h^0} = & -\frac{g_2}{2m_W} \left[m_W^2 \sin(\alpha + \beta) \left[\left(1 - \frac{1}{3} \tan^2 \theta_w\right) (\mathcal{R}_{\tilde{u}})_{jk} (\mathcal{R}_{\tilde{u}}^\dagger)_{ki} \right. \right. \\
& \left. \left. + \frac{4}{3} \tan^2 \theta_w (\mathcal{R}_{\tilde{u}})_{j(k+3)} (\mathcal{R}_{\tilde{u}}^\dagger)_{(k+3)i} \right] \right. \\
& + 2 \frac{\cos \alpha}{\sin \beta} \left[(\mathcal{R}_{\tilde{u}})_{jk} m_{u,k}^2 (\mathcal{R}_{\tilde{u}}^\dagger)_{ki} + (\mathcal{R}_{\tilde{u}})_{j(k+3)} m_{u,k}^2 (\mathcal{R}_{\tilde{u}}^\dagger)_{(k+3)i} \right] \\
& + \frac{\sin \alpha}{\sin \beta} \left[\mu^* (\mathcal{R}_{\tilde{u}})_{j(k+3)} m_{u,k} (\mathcal{R}_{\tilde{u}}^\dagger)_{ki} + \mu (\mathcal{R}_{\tilde{u}})_{jk} m_{u,k} (\mathcal{R}_{\tilde{u}}^\dagger)_{(k+3)i} \right] \\
& \left. + \frac{\cos \alpha}{\sin \beta} \frac{v_2}{\sqrt{2}} \left[(\mathcal{R}_{\tilde{u}})_{j(k+3)} (T_U)_{lk} (\mathcal{R}_{\tilde{u}}^\dagger)_{li} + (\mathcal{R}_{\tilde{u}})_{jk} (T_U^\dagger)_{lk} (\mathcal{R}_{\tilde{u}}^\dagger)_{(l+3)i} \right] \right]. \quad (17)
\end{aligned}$$

The decay width for the process $\tilde{u}_i \rightarrow \tilde{u}_j h^0$ is given by

$$\Gamma(\tilde{u}_i \rightarrow \tilde{u}_j h^0) = \frac{1}{16\pi} \frac{\kappa(m_{\tilde{u}_i}^2, m_{\tilde{u}_j}^2, h^0)}{2m_{\tilde{u}_i}^3} |c_{\tilde{u}_i \tilde{u}_j h^0}|^2. \quad (18)$$

As usual, κ is defined by $\kappa^2(x, y, z) = (x - y - z)^2 - 4yz$.

B Experimental and theoretical constraints

Here we summarize the experimental and theoretical constraints taken into account in the present paper. The constraints on the MSSM parameters from the B-physics experiments and from the Higgs boson search at LHC are shown in Table 4.

The particle discovered most recently at LHC [25, 32, 33] and consistent with the SM Higgs boson we identify as the MSSM Higgs boson h^0 which is indeed SM-like in the decoupling Higgs scenarios considered in our paper. For the mass of the Higgs boson h^0 , we take an average of the central values $((125.3(\text{CMS}) + 126.5(\text{ATLAS}))/2 \simeq 126 \text{ GeV})$ and adding the theoretical uncertainty of $\sim \pm 2 \text{ GeV}$ [34] linearly to the experimental uncertainty of the CMS data at 1.5σ , we take $123 \text{ GeV} < m_{h^0} < 129 \text{ GeV}$. Very recently LHCb has found a first evidence for $B_s \rightarrow \mu^+ \mu^-$ at 3.5σ level and obtained $B(B_s \rightarrow \mu^+ \mu^-) = (3.2 + 1.5/-1.2) \times 10^{-9}$, which is in very good agreement with the SM prediction [35]. They also set a double sided limit at 95% CL: $1.1 \times 10^{-9} < B(B_s \rightarrow \mu^+ \mu^-) < 6.4 \times 10^{-9}$. We have confirmed that this limit is satisfied in all plots presented in this article: for this branching ratio we have obtained numerical results very close to the SM prediction, which is mainly due to the fact that we take a very heavy Higgs mass m_{A^0} ($= 1500 \text{ GeV}$) and that we assume almost no $\tilde{s} - \tilde{b}$ mixing. We do not take the constraint from the recent Babar data on $B(B \rightarrow D^{(*)} \tau \nu)$ [36] because, as pointed out in [37], it is probable that the SM predictions are significantly underestimated and hence that the constraint on $\tan \beta / m_{H^\pm}$ would actually be much weaker than that claimed in [36].

In addition to these constraints we also impose the following experimental constraints:

- (i) The LHC limits on the squark and gluino masses (at 95% CL) [48, 49]

Table 4: Constraints on the MSSM parameters from the B-physics experiments relevant mainly for the mixing between the second and the third generations of squarks and from the limit on the h^0 mass. The fourth column shows constraints at 95% CL obtained by combining the experimental error quadratically with the theoretical uncertainty, except for $B(B_s \rightarrow \mu\mu)$ and m_{h^0} . $R_{B \rightarrow \tau\nu}^{\text{SUSY}} \equiv \frac{B(B^+ \rightarrow \tau^+\nu)_{\text{SUSY}}}{B(B^+ \rightarrow \tau^+\nu)_{\text{SM}}} \approx [1 - ((m_{B^+} \tan \beta)/m_{H^+})^2]^2$ where m_{H^+} is the H^+ mass [38].

Observable	Exp. data	Theor. uncertainty	Constr. (95%CL)
ΔM_{B_s} [ps ⁻¹]	17.725 ± 0.049 (68% CL) [39]	± 3.3 (95% CL) [40]	17.73 ± 3.30
$10^4 \times B(b \rightarrow s\gamma)$	3.37 ± 0.23 (68% CL) [41]	± 0.23 (68% CL) [42]	3.37 ± 0.64
$10^6 \times B(b \rightarrow s l^+ l^-)$ ($l = e$ or μ)	1.60 ± 0.50 (68% CL) [43]	± 0.11 (68% CL) [44]	1.60 ± 1.00
$10^9 \times B(B_s \rightarrow \mu^+ \mu^-)$	< 4.2 (95% CL) [45]		< 4.2
$10^4 \times B(B^+ \rightarrow \tau^+ \nu)$	1.15 ± 0.23 (68% CL) [46]	± 0.25 (68% CL) [47]	$R_{B \rightarrow \tau\nu}^{\text{SUSY}} =$ 0.96 ± 0.54
m_{h^0} [GeV]	125.3 ± 0.64 (68% CL)(CMS), 126.5 (ATLAS) [25]	± 2 [34]	$123 < m_{h^0} < 129$

- In a simplified model: $m_{\tilde{g}} \gtrsim 1050$ GeV, $m_{\tilde{q}} \gtrsim 1380$ GeV (for $m_{\tilde{\chi}_1^0} = 0$), no limit on $m_{\tilde{g}}$ and $m_{\tilde{q}}$ (for $m_{\tilde{\chi}_1^0} \gtrsim 400$ GeV);
- In the context of the CMSSM/mSUGRA: $m_{\tilde{g}} \gtrsim 840$ GeV, $m_{\tilde{q}} \gtrsim 1300$ GeV.

Here $m_{\tilde{q}}$ represents the mass of mass-degenerate 1st and 2nd generation squarks. Note that in general, top-squark and bottom-squark mass limits are significantly weak and quite assumption dependent [48, 50]. Taking into account these limits, we assume a gluino mass larger than 1 TeV in our analysis.

(ii) ATLAS and CMS set limits on $m_{\tilde{\chi}_1^\pm}$ and $m_{\tilde{\chi}_1^0}$ from negative searches for charginos and neutralinos in leptonic final states [51]. Respecting these limits we impose the following conditions: $m_{\tilde{\chi}_1^\pm} \gtrsim 400$ GeV, $m_{\tilde{\chi}_1^0} \gtrsim 200$ GeV.

(iii) The constraint on $(m_{A^0}, \tan \beta)$ from the MSSM Higgs boson searches at LHC [52].

(iv) The experimental limit on SUSY contributions on the electroweak ρ parameter [53]: $\Delta\rho$ (SUSY) < 0.0012 .

Furthermore, we impose the following theoretical constraints from the vacuum stability conditions for the trilinear coupling matrices [54]:

$$|T_{U\alpha\alpha}|^2 < 3 Y_{U\alpha}^2 (M_{Q\alpha\alpha}^2 + M_{U\alpha\alpha}^2 + m_2^2), \quad (19)$$

$$|T_{D\alpha\alpha}|^2 < 3 Y_{D\alpha}^2 (M_{Q\alpha\alpha}^2 + M_{D\alpha\alpha}^2 + m_1^2), \quad (20)$$

$$|T_{U\alpha\beta}|^2 < Y_{U\gamma}^2 (M_{Q\alpha\alpha}^2 + M_{U\beta\beta}^2 + m_2^2), \quad (21)$$

$$|T_{D\alpha\beta}|^2 < Y_{D\gamma}^2 (M_{Q\alpha\alpha}^2 + M_{D\beta\beta}^2 + m_1^2), \quad (22)$$

where $\alpha, \beta = 1, 2, 3$, $\alpha \neq \beta$; $\gamma = \text{Max}(\alpha, \beta)$ and $m_1^2 = (m_{H^\pm}^2 + m_Z^2 \sin^2 \theta_W) \sin^2 \beta - \frac{1}{2} m_Z^2$, $m_2^2 = (m_{H^\pm}^2 + m_Z^2 \sin^2 \theta_W) \cos^2 \beta - \frac{1}{2} m_Z^2$. The Yukawa couplings of the up-type and down-type quarks are $Y_{U\alpha} = \sqrt{2} m_{u_\alpha} / v_2 = \frac{g}{\sqrt{2} m_W \sin \beta} (u_\alpha = u, c, t)$ and $Y_{D\alpha} = \sqrt{2} m_{d_\alpha} / v_1 = \frac{g}{\sqrt{2} m_W \cos \beta} (d_\alpha = d, s, b)$, with m_{u_α} and m_{d_α} being the running quark masses at the weak scale and g being the SU(2) gauge coupling. All soft-SUSY-breaking parameters are also assumed to be given at the weak scale. As SM parameters we take $m_W = 80.4$ GeV, $m_Z = 91.2$ GeV and the on-shell top-quark mass $m_t = 173.3$ GeV [55]. We have found that our results shown are fairly insensitive to the precise value of m_t .

We take into account all constraints listed in this section in all plots presented in this article. The constraints on the QFV parameters from $B(b \rightarrow s\gamma)$, ΔM_{B_s} , m_{h^0} , and the vacuum stability conditions are especially important for this study. We use the public code SPheno v3.1 [22, 23] in the computation of the observables except for cross sections (i. e. physical masses, decay branching ratios, $\Delta_{M_{B_s}}$ and $\Delta_\rho(\text{SUSY})$) in this article.

References

- [1] A. J. Buras *et al.*, Phys. Lett. B **500** (2001) 161 [arXiv:hep-ph/0007085].
- [2] G. D'Ambrosio, G. F. Giudice, G. Isidori and A. Strumia, Nucl. Phys. B **645** (2002) 155 [arXiv:hep-ph/0207036].
- [3] A. L. Kagan, G. Perez, T. Volansky and J. Zupan, Phys. Rev. D **80** (2009) 076002 [arXiv:0903.1794, hep-ph].
- [4] J. Beringer *et al.* [Particle Data Group Collaboration], Phys. Rev. D **86** (2012) 010001.
- [5] G. Hiller and Y. Nir, JHEP **0803** (2008) 046 [arXiv:0802.0916 [hep-ph]].
- [6] G. Hiller, J. S. Kim and H. Sedello, Phys. Rev. D **80** (2009) 115016 [arXiv:0910.2124 [hep-ph]].
- [7] M. Muhlleitner and E. Poppo, JHEP **1104** (2011) 095 [arXiv:1102.5712 [hep-ph]].
- [8] G. Bozzi, B. Fuks, B. Herrmann and M. Klasen, Nucl. Phys. B **787** (2007) 1 [arXiv:0704.1826 [hep-ph]].
- [9] B. Fuks, B. Herrmann and M. Klasen, Nucl. Phys. B **810** (2009) 266 [arXiv:0808.1104 [hep-ph]].
- [10] A. Bartl *et al.*, Phys. Lett. B **698** (2011) 380 [Erratum-ibid. B **700** (2011) 390] [arXiv:1007.5483 [hep-ph]].
- [11] M. Bruhnke, B. Herrmann and W. Porod, JHEP **1009** (2010) 006 [arXiv:1007.2100 [hep-ph]].

- [12] T. Hurth and W. Porod, JHEP **0908** (2009) 087 [arXiv:0904.4574, hep-ph].
- [13] A. Bartl *et al.*, Phys. Lett. B **679** (2009) 260 [arXiv:0905.0132 [hep-ph]].
- [14] A. Bartl *et al.*, Phys. Rev. D **84** (2011) 115026 [arXiv:1107.2775 [hep-ph]].
- [15] B. Fuks, B. Herrmann and M. Klasen, Phys. Rev. D **86** (2012) 015002 [arXiv:1112.4838 [hep-ph]].
- [16] A. Bartl, W. Majerotto and W. Porod, Z. Phys. C **64** (1994) 499 [Erratum-ibid. C **68** (1995) 518].
- [17] A. Bartl *et al.*, Phys. Lett. B **435** (1998) 118 [hep-ph/9804265].
- [18] A. Djouadi, J. L. Kneur and G. Moultaka, Nucl. Phys. B **569** (2000) 53 [hep-ph/9903218].
- [19] B. C. Allanach *et al.*, Comput. Phys. Commun. **180** (2009) 8 [arXiv:0801.0045 [hep-ph]].
- [20] F. Gabbiani, E. Gabrielli, A. Masiero and L. Silvestrini, Nucl. Phys. B **477** (1996) 321 [hep-ph/9604387].
- [21] J. A. Aguilar-Saavedra *et al.*, Eur. Phys. J. C **46** (2006) 43 [hep-ph/0511344].
- [22] W. Porod, Comput. Phys. Commun. **153** (2003) 275 [hep-ph/0301101].
- [23] W. Porod and F. Staub, Comput. Phys. Commun. **183** (2012) 2458 [arXiv:1104.1573 [hep-ph]].
- [24] F. Staub, T. Ohl, W. Porod and C. Speckner, Comput. Phys. Commun. **183** (2012) 2165 [arXiv:1109.5147 [hep-ph]].
- [25] CMS data: J. Incandela, plenary talk at 36th International Conference on High Energy Physics, Melbourne, Australia, 4-11 July 2012; ATLAS data: R. Hawking, plenary talk at 36th International Conference on High Energy Physics, Melbourne, Australia, 4-11 July 2012.
- [26] F. Brümmer, S. Kraml and S. Kulkarni, JHEP **1208** (2012) 089 [arXiv:1204.5977 [hep-ph]].
- [27] A. Arbey, M. Battaglia, A. Djouadi and F. Mahmoudi, JHEP **1209** (2012) 107 [arXiv:1207.1348 [hep-ph]].
- [28] R. Benbrik *et al.*, arXiv:1207.1096 [hep-ph].
- [29] W. Beenakker, R. Höpker, M. Spira, P. M. Zerwas, JHEP **08** (2010), 098 [arXiv:1006.4771 [hep-ph]].

- [30] T. Hahn, Comput. Phys. Commun. **140** (2001), 418 [arXiv:hep-ph/0012260].
- [31] T. Hahn and C. Schappacher, Comput. Phys. Commun. **143** (2002), 54 [arXiv:hep-ph/0105349].
- [32] G. Aad *et al.* [ATLAS Collaboration], Phys. Lett. B **710** (2012) 49 [arXiv:1202.1408 [hep-ex]].
- [33] S. Chatrchyan *et al.* [CMS Collaboration], Phys. Lett. B **710** (2012) 26 [arXiv:1202.1488 [hep-ex]].
- [34] S. Heinemeyer, O. Stal and G. Weiglein, Phys. Lett. B **710** (2012) 201 [arXiv:1112.3026 [hep-ph]].
- [35] J. Albrecht, plenary talk at Hadron Collider Physics Symposium 2012 (HCP2012), Nov 12-16, 2012, Kyoto, Japan.
- [36] J. P. Lees *et al.* [BaBar Collaboration], Phys. Rev. Lett. **109** (2012) 101802 [arXiv:1205.5442 [hep-ex]]; G. D. Nardo, parallel talk at 36th International Conference on High Energy Physics, Melbourne, Australia, 4-11 July 2012.
- [37] M. Danilov, parallel talk at 36th International Conference on High Energy Physics, Melbourne, Australia, 4-11 July 2012.
- [38] W. -S. Hou, Phys. Rev. D **48** (1993) 2342.
- [39] S. Vecchi, parallel talk at 36th International Conference on High Energy Physics, Melbourne, Australia, 4-11 July 2012.
- [40] M. S. Carena *et al.*, Phys. Rev. D **74** (2006) 015009 [hep-ph/0603106]; see also P. Ball and R. Fleischer, Eur. Phys. J. C **48** (2006) 413 [hep-ph/0604249].
- [41] S. Stone, plenary talk at 36th International Conference on High Energy Physics, Melbourne, Australia, 4-11 July 2012.
- [42] M. Misiak *et al.*, Phys. Rev. Lett. **98** (2007) 022002 [hep-ph/0609232].
- [43] M. Iwasaki *et al.* [Belle Collaboration], Phys. Rev. D **72** (2005) 092005 [hep-ex/0503044]; B. Aubert *et al.* [BABAR Collaboration], Phys. Rev. Lett. **93** (2004) 081802 [hep-ex/0404006].
- [44] T. Huber, T. Hurth and E. Lunghi, Nucl. Phys. B **802** (2008) 40 [arXiv:0712.3009 [hep-ph]].
- [45] M. Perrin-Terrin, parallel talk at 36th International Conference on High Energy Physics, Melbourne, Australia, 4-11 July 2012.
- [46] R. Barbieri, summary talk at 36th International Conference on High Energy Physics, Melbourne, Australia, 4-11 July 2012.

- [47] K. Trabelsi, plenary talk at ICHEP2010, PoS (ICHEP 2010) 566.
- [48] A. Parker, plenary talk at 36th International Conference on High Energy Physics, Melbourne, Australia, 4-11 July 2012; M. Backes, parallel talk at the same conference.
- [49] G. Aad *et al.* [ATLAS Collaboration], arXiv:1208.0949 [hep-ex] (submitted to Phys. Rev. D); G. Aad *et al.* [ATLAS Collaboration], arXiv:1208.4688 [hep-ex] (submitted to Phys. Rev. D); G. Aad *et al.* [ATLAS Collaboration], ATLAS-CONF-2012-103; G. Aad *et al.* [ATLAS Collaboration], arXiv:1206.1760 [hep-ex] (submitted to JHEP); S. Chatrchyan *et al.* [CMS Collaboration], arXiv:1206.3949 [hep-ex] (submitted to Phys. Lett. B); S. Chatrchyan *et al.* [CMS Collaboration], <http://cdsweb.cern.ch/record/1460434>; S. Chatrchyan *et al.* [CMS Collaboration], <http://cdsweb.cern.ch/record/1460433>; S. Chatrchyan *et al.* [CMS Collaboration], arXiv:1208.4859 [hep-ex] (submitted to Phys. Rev. D); S. Chatrchyan *et al.* [CMS Collaboration], arXiv:1205.6615 [hep-ex] (submitted to Physical Review Letters); S. Chatrchyan *et al.* [CMS Collaboration], arXiv:1204.3774 [hep-ex] (submitted to Physics Letters B).
- [50] A. Cakir [CMS Collaboration], arXiv:1211.6289 [hep-ex]; G. Aad *et al.* [ATLAS Collaboration], arXiv:1209.2102 [hep-ex] (submitted to Phys. Lett. B); G. Aad *et al.* [ATLAS Collaboration], arXiv:1208.4305 [hep-ex] (submitted to Eur. Phys. J. C); G. Aad *et al.* [ATLAS Collaboration], arXiv:1208.2590 [hep-ex]; G. Aad *et al.* [ATLAS Collaboration], arXiv:1208.1447 [hep-ex] (submitted to Physical Review Letters); G. Aad *et al.* [ATLAS Collaboration], arXiv:1207.4686 [hep-ex] (submitted to Eur. Phys. J. C); G. Aad *et al.* [ATLAS Collaboration], arXiv:1203.6193 [hep-ex] (submitted to Physical Review D); G. Aad *et al.* [ATLAS Collaboration], arXiv:1203.5763 [hep-ex] (submitted to Physical Review Letters); G. Aad *et al.* [ATLAS Collaboration], Phys. Rev. Lett. 108 (2012) 181802 [arXiv:1112.3832 [hep-ex]].
- [51] G. Aad *et al.* [ATLAS Collaboration], arXiv:1208.3144 [hep-ex]; S. Chatrchyan *et al.* [CMS Collaboration], [arXiv:1209.6620 [hep-ex]].
- [52] S. Chatrchyan *et al.* [CMS Collaboration], Phys. Lett. B **713** (2012) 68 [arXiv:1202.4083 [hep-ex]].
- [53] G. Altarelli, R. Barbieri and F. Caravaglios, Int. J. Mod. Phys. A **13** (1998) 1031 [hep-ph/9712368].
- [54] J. A. Casas and S. Dimopoulos, Phys. Lett. B **387** (1996) 107 [hep-ph/9606237].
- [55] E. Shabalina, plenary talk at ICHEP2010, PoS (ICHEP 2010) 561.